Automated Algorithm for MFRSR Data Analysis

M. D. Alexandrov and B. Cairns
Columbia University and
National Aeronautics and Space Administration
Goddard Institute for Space Studies
New York, New York

A. A. Lacis and B. E. Carlson
National Aeronautics and Space Administration
Goddard Institute for Space Studies
New York, New York

A. Marshak
National Aeronautics and Space Administration
Goddard Space Flight Center
Greenbelt, Maryland

We present a substantial upgrade of our previously developed multi-filter rotating shadowband (MFRSR) data analysis algorithm (Alexandrov et al. 2002). For the new version an automated cloud screening procedure (Alexandrov et al. 2004) has been designed and a bimodal aerosol particle size distribution model is used defined by a variable fine mode size and a ratio between the fine and coarse modes.

Automated Cloud Screening Algorithm

The algorithm uses single channel direct beam measurements and is based on variability analysis of retrieved optical thickness. To quantify this variability the inhomogeneity parameter ε is used. This parameter is commonly used for cloud remote sensing and modeling, but not for cloud screening. For our purposes we had to modify it as follows

$$\varepsilon' = \exp(<\ln \tau'>)/<\tau'>,$$

where

$$\tau' = \tau - <\tau> + \tau_{const}$$

Here τ is the measured optical thickness, <...> denote moving average (with 15 data points = 5 min window), τ_{const} is a typical aerosol optical thickness (AOT) value (we select 0.2). In addition to this an adjustable enveloping technique is applied to control strictness of the selection method. A typical example of the algorithm's results for a real MFRSR daily dataset is shown in Figure 1. The key advantages of this technique are its objectivity, computational efficiency and the ability to detect short

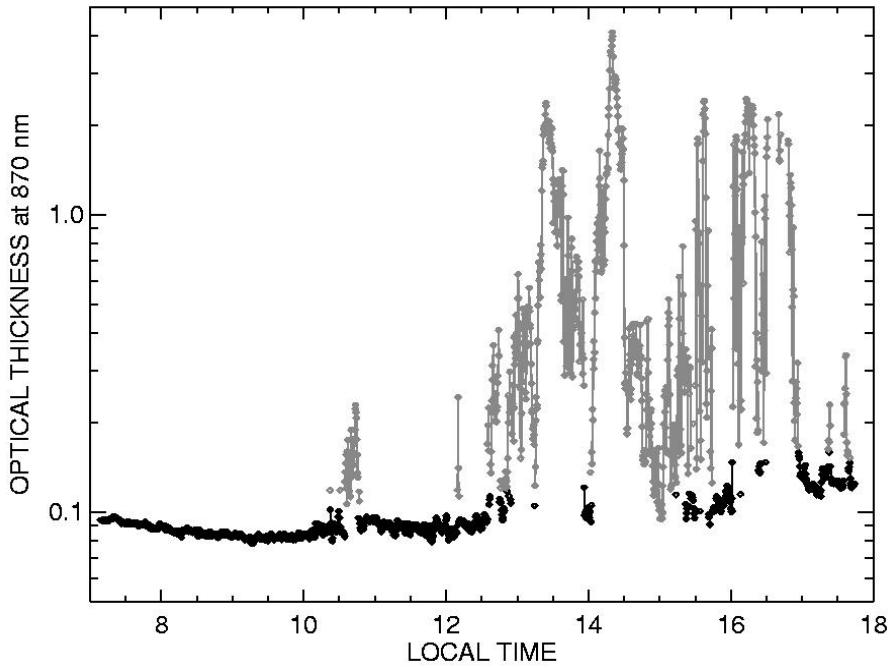

Figure 1. Cloud screening results on the optical thickness plot (in log scale) for in 870 nm MFRSR channel measured on September 11, 2000, at E13 Extended Facility. Cloudy parts of the data are shown in grey, clear-sky parts - in black.

clear-sky intervals under broken cloud cover conditions. Moreover, it does not require any knowledge of the instrument calibration. The performance of the method has been compared with that of Aerosol Robotic Network (AERONET) cloud screening algorithm (Figure 2). It has been also tested on simulated data.

Retrieval Algorithm

A bimodal gamma distribution is adopted as aerosol particle size model. A size of the fine mode particles and a ratio between optical thicknesses of the two modes are retrievable. The coarse mode has a fixed particle size of 1.5 μm. In the case when the fine mode size exceeds 0.5 μm the contribution of the two modes into total AOT become hardly distinguishable within the visible spectral range. In this situation and/or when the ratio between modes become unphysical a retrieval with a monomodal size distribution is performed and the retrieved size is later classified as fine or coarse. Besides the AOT and the fine mode size, the products of our analysis include time series of column amounts of ozone and nitrogen dioxide. Determination of the instrument's calibration constants from the data is a part of the retrieval process.

Our algorithm is applied simultaneously to a set of daily MFRSR records covering at least a month of measurements and runs level by level: first all days are cloud screened, then all 870 nm records are calibrated using compatibility between the direct and diffuse measurements, etc. This approach allows for stabilization of the daily calibration constants on each level using a robust smoothing technique.

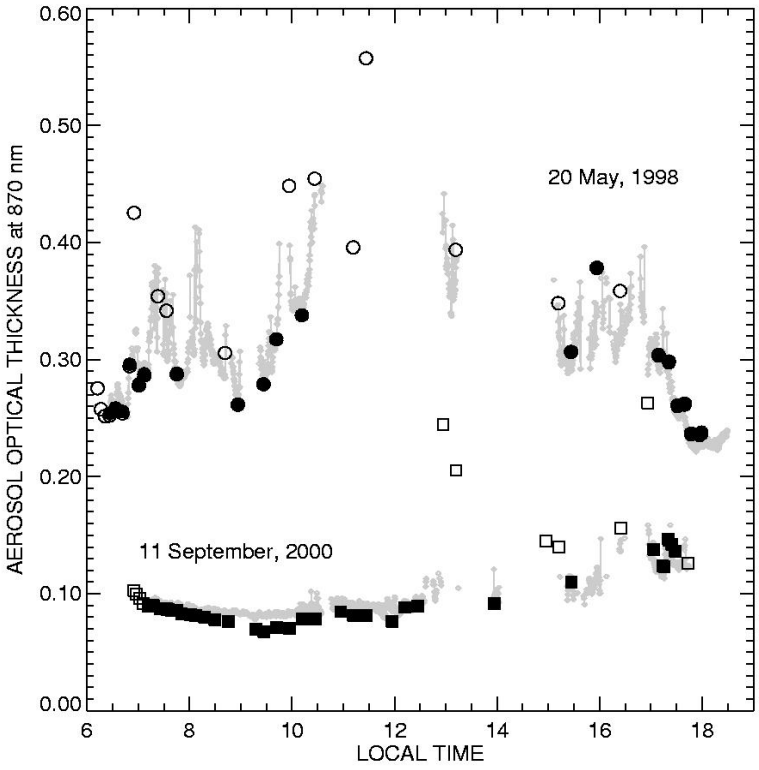

Figure 2. Comparison with AERONET cloud screening. The cloud-screened MFRSR data for September 11, 2000, and May 20, 1998 (smoke event), are shown in grey. The corresponding level 1.0 AERONET data points (after rough initial cloud screening) are depicted by circles for May 20, 1998, and by squares for September 11, 2000. The data points selected for level 1.5 cloud-screened dataset are filled with black

The separation of the total AOT into fine and coarse parts requires high data quality. Thus, some noise filtering and other regularization techniques are applied to the data in order to make this separation possible. To make sure that this part of our algorithm works properly, we compared (see Figure 3) its results with the total, fine, and coarse AOTs obtained from AERONET almucantar retrievals for 870, 670, and 440 nm channels (the latter interpolated for MFRSR) based on both spectral and angular dependences of the scattered radiation. AERONET's CIMEL sunphotometer provided the data is colocated with MFRSR at the Southern Great Plains (SGP) central facility. For a clear day 4 almucantar scan retrievals are available. While the agreement in totals is better than in fine and coarse AOT separately, we consider these results successful, taking into account the difference in the measurements and aerosol model assumptions.

Geographical Variations of Aerosol Type Across the SGP Site

Analysis of a year 2000 MFRSR dataset from all SGP Extended Facilities revealed pronounced geographical differences in the retrieved size of fine mode aerosols. Figure 4 presents three characteristic types (we called them A, B, and C) of the fine mode effective radius variability, that, we

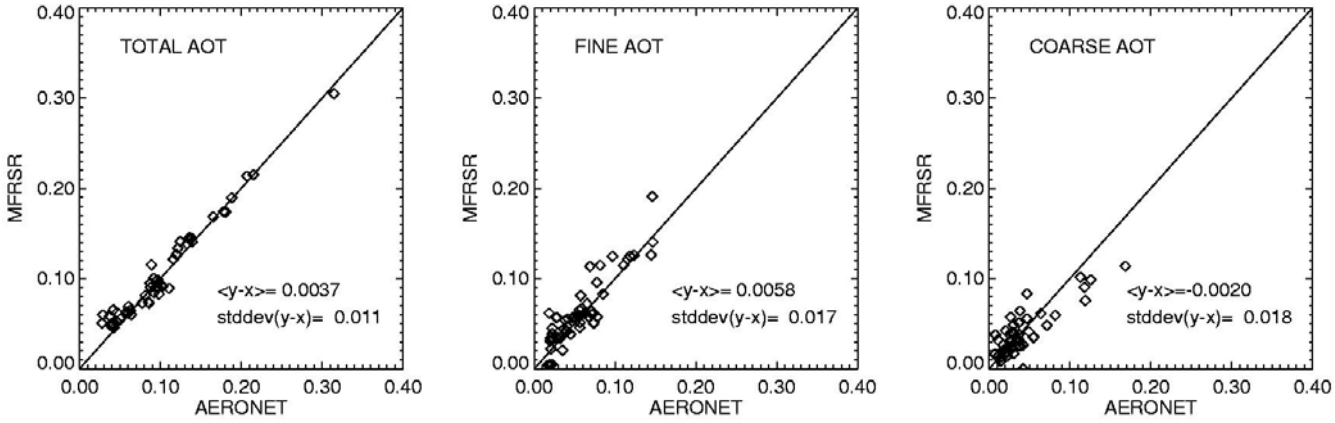

Figure 3. Comparison between MFRSR-derived AOTs at 870 nm wavelength (total, fine, and coarse) and those from AERONET almucantar scan analysis. Top: daily examples (AERONET values are shown by large diamonds). Bottom: scatterplot for all measurements used from May 1 to June 18, 2003 (22 days, 52 datapoints). The comparison for 670 and 440 nm CIMEL channels shows similar results. The MFRSR and CIMEL sunphotometers are located at the SGP site central facility.

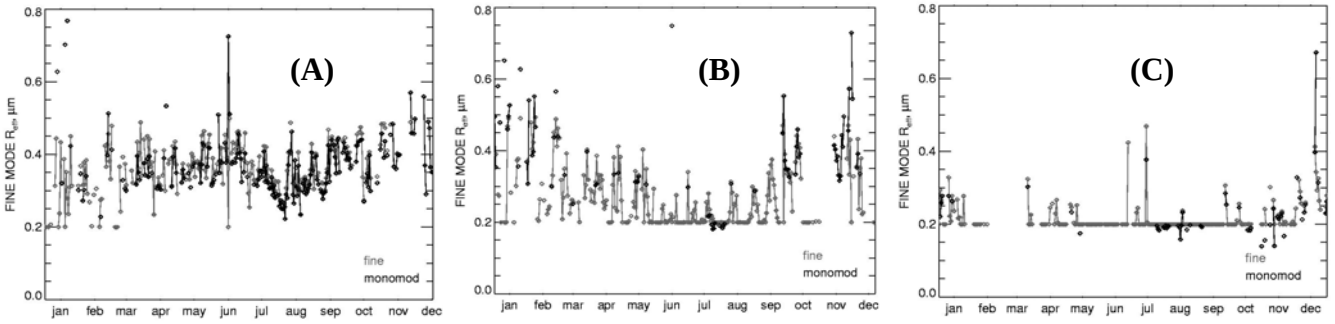

Figure 4. Time series of daily mean fine mode effective particle radius for SGP Extended Facilities E2, E4, and E24 (left to right) for the year 2000. They illustrate the corresponding three characteristic types of variability: **A**. NE and SW of the site, large 0.3 - 0.4 μm particles with no seasonal trends; **B**. NW and center, intermediate type with larger particles in Winter; **C**. SE, very small fine mode particles (smaller than the retrieval threshold of 0.2 μm). The values of monomodal r_{eff} <0.2 μm are artifacts due to imperfect instrument angular response at large zenith angles and should be discarded.

suggest, indicate different aerosol species. The areas of domination of these behavior types are shown on the SGP site map in Figure 5. Type A characteristic to the north-east and south-west of the site `corresponds to larger 0.3-0.5 μm particles with no significant seasonality in their size. Type C dominating the south-east, corresponds to very small aerosol particles with r_{eff} less or equal to our detection limit 0.2 μm. Type B intermediate between A and B is encountered in the north-west and the central parts of SGP. In this aerosol mass both small and larger particles are present, while the latter exhibit seasonality with maximum size in winter. To explain these differences we used the NO_3/SO_4 ion concentration ratios obtained from National Atmospheric Deposition Program/National Trends Network (NADP/NTN, http://nadp.sws.uiuc.edu) precipitation monitoring sites in Oklahoma, Kansas, and the neighboring states. The result of interpolation between the mean values for the year 2000 is shown as a

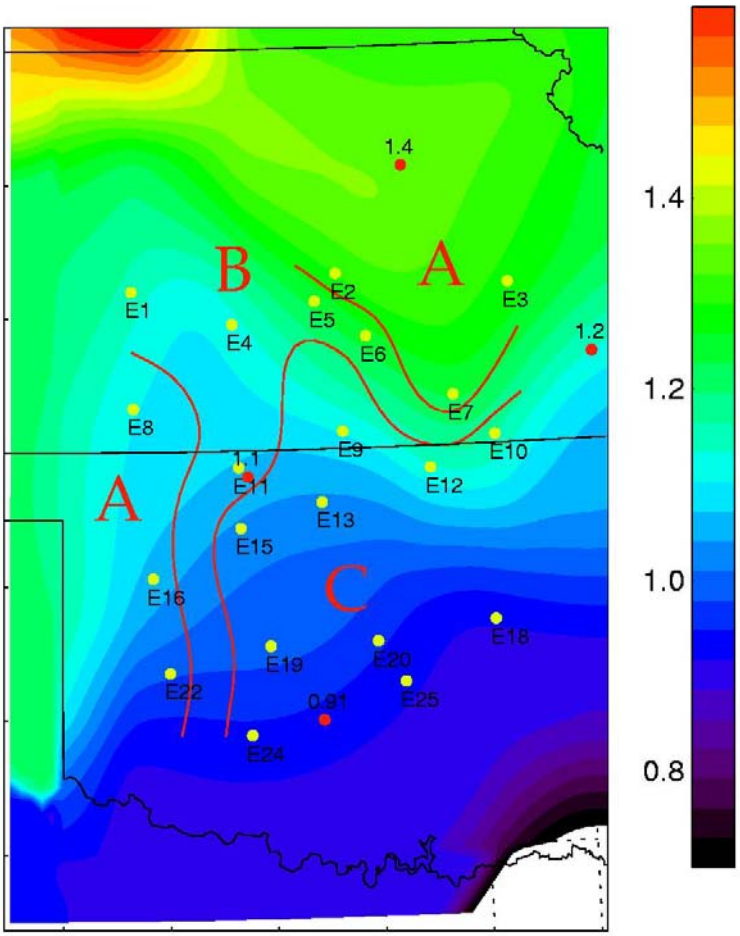

Figure 5. Contour plot of the NO_3/SO_4 ion concentration ratios (mean values for the year 2000) obtained from NADP/NTN precipitation monitoring sites (some of them are shown by open circles). The types A and B of aerosol fine particles (see Figure 4) appear to correspond to nitrate-dominated areas, while the smaller particles (type C) are encountered in the sulfate-dominated south-east of the SGP site.

contour plot in Figure 5. This plot shows a trend corresponding to domination of nitrates in A-zones (especially in the north) opposed to domination of sulfates in the C-zone in the south-east of the site. These results are in agreement with the fact that nitrate aerosol particles are generally larger than their sulfate counterparts.

Tracing Pinatubo Voulcanic Aerosols

To check qualitative consistence of our retrievals with known aerosol events we considered 1993 to 1997 dataset from SGP central facility. This dataset includes measurements during the aftermath of the Mt. Pinatubo eruption in June 1991 that induced an enormous population of large aerosol particles in the stratosphere which remained there for a few years after the eruption. This effect has been well-documented by a variety of sun-photometric, lidar, in situ, and satellite studies. Figure 6 shows our

retrievals for 1993 to 1997 period. It is seen that our algorithm attributed Pinatubo aerosols to the coarse mode. The coarse AOT exhibits a decrease during 1993 to 1995 and shows practically no seasonal variations. In contrast to this the fine mode AOT shows no visible impact of the Pinatubo event, while exhibits strong seasonal behavior with AOT maxima in summer time.

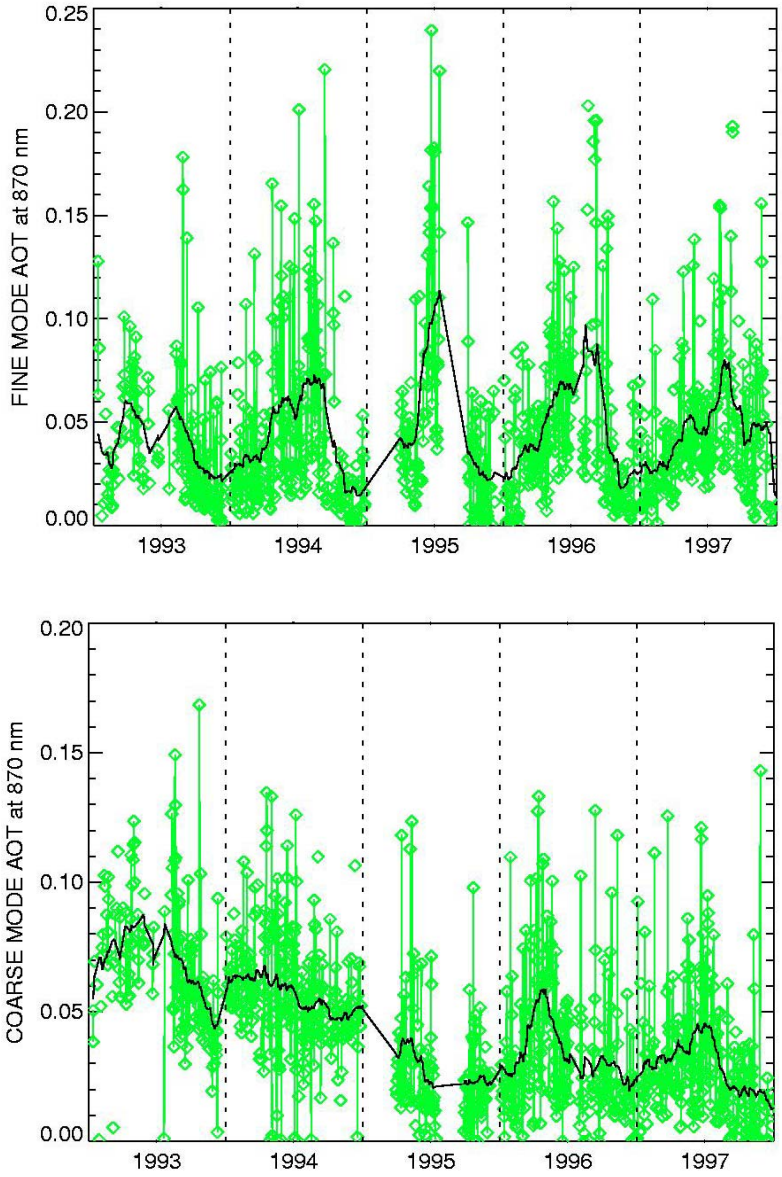

Figure 6. Time series of daily mean fine (top) and coarse (bottom) AOT retrieved from SGP central facility MFRSR dataset for 1993 to 1997. The strong 1993 to 1995 trend in the coarse AOT corresponds to dissipation of Mt. Pinatubo voulcanic aerosols. In distinction to the coarse mode, the fine mode AOT shows no interannual trends, while exhibits strong seasonal cycles with maxima in summer.

Corresponding Author

Mikhail Alexandrov, malexandrov@giss.nasa.gov, (212) 678-5548

References

Alexandrov, M., A. A. Lacis, B. E. Carlson, and B. Cairns, 2002: Remote sensing of atmospheric aerosols and trace gases by means of multifilter rotating shadowband radiometer. Part I: Retrieval Algorithm. *J. Atmos. Sci*., **59**, 524–543.

Alexandrov, M. D., A. Marshak, B. Cairns, A. A. Lacis, and B. E. Carlson, 2004: Automated cloud screening algorithm for MFRSR data. *Geophys. Res. Lett*., **31**, L04118, doi:10.1029/2003GL019105.